A TURBULENCE MODULE FOR THE NPARC CODE

J. Zhu * and T.-H. Shih
Center for Modeling of Turbulence and Transition
ICOMP, OAI, NASA Lewis Research Center
Cleveland, Ohio 44135

Abstract

A turbulence module is developed for the 2D version of the NPARC code which is currently restricted to planar or axisymmetric flows without swirling. Four turbulence models have been built into the module: Baldwin-Lomax, Chien, Shih-Lumley and CMOTT models. The first is a mixing-length eddy-viscosity model which is mainly used for initialization of computational fields and the last three are the low Reynolds number two-equation models. Unlike Chien's model, both the Shih-Lumley and CMOTT models do not involve the dimensionless wall distance y^+, an advantage for separated flow calculations. Contrary to the NPARC and most other compressible codes, the non-delta form of transport equations is used which leads to a simpler linearization and is more effective than using the delta form in ensuring the positiveness of the turbulent kinetic energy and its dissipation rate. To reduce numerical diffusion while maintaining necessary stability, a second-order accurate and bounded scheme is used for the convective terms of the turbulent transport equations. This scheme is implemented in a deferred correction manner so that the main coefficients of the resulting difference equations are always positive, thus making the numerical solution process unconditionally stable. The system of equations are solved via a decoupled method and by the alternating direction TDMA of Thomas. The module can be easily linked to the NPARC code for turbulent flow calculations.

1. Introduction

It has been long recognized that there is a gap between turbulence model developers and CFD users. The former mainly use simple flows to verify new modeling concepts and evaluate the resulting models, while the latter are usually reluctant to implement and test new, more advanced turbulence models until they see such models showing good performance for a wide range of complex flow situations.

In order to bridge this gap, we have developed turbulence modules for CFD codes used in industry. Under the widely used Boussinesq's isotropic eddy-viscosity concept, the Reynolds-averaged equations governing turbulent flows are of the same form as those governing laminar flows, except that the laminar viscosity μ is replaced by the effective viscosity

$$\mu_{eff} = \mu + \mu_t \tag{1}$$

Therefore, a mean flow solver can be used to calculate turbulent flows once the turbulent eddy-viscosity μ_t is available. The module is written in a self-contained manner so that the user can use any turbulence model in the module without concern as to how it is implemented and solved. The input to the module are the mean flow variables, boundary and geometric information which are to be provided by a mean flow solver. The output of the module are the turbulent eddy-viscosity μ_t and relevant turbulent source terms which are needed for the mean flow calculation. Here the turbulent source terms exist only for more sophisticated turbulence models beyond the level of isotropic eddy-viscosity models. For most CFD codes, especially those for compressible flow calculations, the laminar viscosity μ is a variable not a constant. In this case, few changes are required for a mean flow solver to use the turbulence module. The interaction between the mean flow solver and the turbulence module will give the final turbulent flow solution, as shown in Fig.1. With the aid of the modules, turbulence model developers can also take the advantage of the well-established and sophisticated CFD codes to test turbulence models for a variety of complex flows which are intractable with simple research codes.

The NPARC code has been extensively used in the U.S. aerospace and aeropropulsion communities. The code can handle very complicated geometries. However until recently, only algebraic models such as

*Member AIAA

the Thomas and Baldwin-Lomax models have been available in the NPARC code for turbulent flow simulations. The Chien's low Reynolds number K-ϵ model[1] with modifications for compressibility has been available in the 2D version but was not successfully installed in the 3D version. Another K-ϵ model (the NPARC 1.0 K-ϵ model) was installed in both the 2D and 3D versons but has not provided desirable accuracy and stability. Recently, the two-equation turbulence model in the NAPRC code (both the 2D and 3D versions) has been modified so that the model is based on the low Reynolds number K-ϵ model of Chien and no longer on the NPARC 1.0 K-ϵ model. Stability enhancements and a new inflow boundary condition for the turbulent quantities were also added to the K-ϵ model. Comparisons of the NPARC solutions obtained using the previous and newly installed models with experimental data indicated that the Chien's K-ϵ model installed improves the capability of the NPARC code for propulsion turbulent flow calculations[2].

In the module developed for the NPARC code, the three low Reynolds number K-ϵ turbulence models have been implemented: Chien[1], Shih-Lumley[3] and CMOTT models. The Baldwin-Lomax mixing-length model is also included in the module, but it is mainly for initializing computational fields. Chien's model is one of the well-known low Reynolds number K-ϵ models. However, it has some undesirable deficiencies. First, a near wall pseudo-dissipation rate is introduced to remove the singularity in the dissipation rate equation at the wall. The definition of the near wall pseudo-dissipation rate is quite arbitrary. Second, the model constants are different from those of the standard K-ϵ model[4], making the near wall model less capable of handling flows containing both high Reynolds number turbulence and near wall turbulence, which is often the case for practical flows. Patel et al.[5] require as the first criterion, the ability of the near wall models to be able to predict turbulent free shear flows. Third, the dimensionless wall distance y^+ is used in the damping function f_μ for the eddy-viscosity. Because the y^+ involves the friction velocity u_τ which is equal to zero at separation or reattachment points, any model using y^+ may have difficulties for separated flows. The Shih-Lumley and CMOTT models are free of these deficiencies. The two models differ from one another in the C_μ formulation, one using the standard constant and the other a new formulation. The new C_μ has the following desirable features: (a) It is derived from a rigorous realizability analysis[6] that requires the non-negativity of the turbulent normal stresses and Schwarz' inequality between any fluctuating quantities. As a result, unlike most of the existing models, it satisfies the realizability conditions. (b) It accounts for the effect of the mean deformation rate by which the eddy-viscosity will be significantly reduced to an adequate level to mimic complex flow structures. (c) It is easier to use, as compared with other formulations. Simplicity is of great value for practical engineering applications. Successful applications of this new C_μ can be found in Shih et al.[6,7].

Turbulence model equations require special treatment to ensure numerical realizability such as the positiveness of the turbulent kinetic energy and its dissipation rate. They are also often of source-dominate nature, which makes the linearization of source terms crucial for computational stability. Due to these considerations, we use the non-delta form of the transport equations in the module, which is contrary to the NPARC code as well as most other compressible codes. The non-delta form leads to simpler linearization and is more effective to ensure the positiveness of the turbulent kinetic energy and its dissipation rate than the delta form. For simplicity and also due to the fact that the coupling between the turbulence model equations is, in general, not very critical for the overall solution process, these equations are solved in a decoupled manner. The discretization of the convection terms is another important issue. The key point is to use a scheme which reduces numerical or false diffusion to such a level that it will not obscure the real viscous process, while maintaining necessary stability. Here, a hybrid linear/parabolic approximation (HLPA) scheme of second-order accuracy[8] is used. It is shown[9] that the HLPA scheme is capable of yielding low diffusive and always bounded solutions, and reconciles quite well the conflicting requirements of stability, accuracy and algorithmic simplicity.

In what follows, we will present the details of the module and demonstrate how it is linked to the NPARC code. Application of the module will be reported in another paper[10].

2. Turbulence Models

In accordance with the NPARC code, a non-dimensional form of equations is adopted. The three low Reynolds number two-equation turbulence models built into the module have the following common form in which the Reynolds stresses $\tau_{ij}(=-\rho\overline{u_i u_j})$ are calculated by

$$\tau_{ij} = R_e^{-1}\mu_t(U_{i,j} + U_{j,i} - \frac{2}{3}U_{k,k}) - \frac{2}{3}\rho K\delta_{ij} \quad (2)$$

where R_e is the reference Reynolds number. The turbulent eddy viscosity μ_t, the turbulent kinetic energy K and its dissipation rate ϵ are calculated by the following equations

$$\mu_t = R_e f_\mu C_\mu \rho \frac{K^2}{\epsilon} \tag{3}$$

$$\begin{aligned}&(\rho K)_{,t} + [\rho U_j K - R_e^{-1}(\mu + \frac{\mu_t}{\sigma_K})K_{,j}]_{,j} \\ &= P - \rho\epsilon + D\end{aligned} \tag{4}$$

$$\begin{aligned}&(\rho\epsilon)_{,t} + [\rho U_j \epsilon - R_e^{-1}(\mu + \frac{\mu_t}{\sigma_\epsilon})\epsilon_{,j}]_{,j} \\ &= f_1 C_1 \frac{\epsilon}{K} P - f_2 C_2 \rho \frac{\epsilon^2}{K} + E\end{aligned} \tag{5}$$

where

$$P = \tau_{ij} U_{i,j} \tag{6}$$

$$f_1 = 1 \tag{7}$$

$$f_2 = 1 - 0.22\exp[-(R_t/6)^2] \tag{8}$$

$$R_t = \frac{R_e \rho K^2}{\mu\epsilon} \tag{9}$$

P is the turbulent production. For high Reynolds number models, $f_\mu = f_1 = f_2 = 1$ and $D = E = 0$. The differences in the three models are given below:

1) Chien's K-ϵ model.

$$\begin{aligned}&C_\mu = 0.09,\ C_1 = 1.35,\ C_2 = 1.8 \\ &\sigma_K = 1,\ \sigma_\epsilon = 1.3\end{aligned} \tag{10}$$

$$\begin{aligned}&f_\mu = 1 - \exp(-0.0115 y^+) \\ &y^+ = \frac{R_e \rho u_\tau y_n}{\mu}\end{aligned} \tag{11}$$

$$D = -2R_e^{-1}\mu \frac{K}{y_n^2} \tag{12}$$

$$E = -\frac{2R_e^{-1}\mu\epsilon}{y_n^2}\exp(-0.5y^+) \tag{13}$$

At the wall, the values of K and ϵ are both set to zero.

2) Shih-Lumley's K-ϵ model.

$$\begin{aligned}&C_\mu = 0.09,\ C_1 = 1.44,\ C_2 = 1.92 \\ &\sigma_K = 1,\ \sigma_\epsilon = 1.3\end{aligned} \tag{14}$$

$$\begin{aligned}&f_\mu = [1 - \exp(-a_1 R_k - a_3 R_k^3 - a_5 R_k^5)]^{1/2} \\ &R_K = \frac{R_e \rho K^{1/2} y_n}{\mu}\end{aligned} \tag{15}$$

$$a_1 = 1.7 * 10^{-3},\ a_3 = 10^{-9},\ a_5 = 5 * 10^{-10}$$

$$D = 0 \tag{16}$$

$$E = \frac{\mu\mu_t}{\rho R_e^2} S_{,i} S_{,i} \tag{17}$$

$$S = \sqrt{2 S_{ij}^* S_{ji}^*} \tag{18}$$

$$S_{ij}^* = \frac{1}{2}(U_{i,j} + U_{j,i}) - \frac{1}{3} U_{k,k}\delta_{ij} \tag{19}$$

The wall boundary conditions for K and ϵ are

$$K = 0.250 u_\tau^2 \tag{20}$$

$$\epsilon = 0.251 R_e \frac{\rho u_\tau^4}{\mu} \tag{21}$$

3) CMOTT K-ϵ model. This model is the same as the Shih-Lumley model, except that C_μ is calculated by

$$C_\mu = \min[0.09,\ (A_0 + A_s U^* K/\epsilon)^{-1}] \tag{22}$$

where

$$A_0 = 4, \quad A_s = \sqrt{6}\cos\phi \tag{23}$$

$$U^* = \sqrt{S_{ij}^* S_{ij}^* + \Omega_{ij}\Omega_{ij}} \tag{24}$$

$$\phi = \frac{1}{3} arc\cos(\sqrt{6}W), \quad W = \frac{S_{ij}^* S_{jk}^* S_{ki}^*}{(S^*)^3} \tag{25}$$

$$S^* = \sqrt{S_{ij}^* S_{ij}^*}, \quad \Omega_{ij} = \frac{1}{2}(U_{i,j} - U_{j,i}) \tag{26}$$

In the above formulas, y_n refers to the normal distance from the wall.

3. Calculation Procedure

3.1 General Form of Turbulence Equations

The turbulent transport equations (4) and (5) in general curvilinear coordinates (ξ, η) may be written in the following form:

$$\begin{aligned}&\partial_t(rJ^{-1}\rho\phi) + \partial_\xi(rJ^{-1}\rho U\phi) + \partial_\eta(rJ^{-1}\rho V\phi)\\&- \partial_\xi(rJ^{-1}\mu_\phi\nabla\xi\cdot\nabla\phi) - \partial_\eta(rJ^{-1}\mu_\phi\nabla\eta\cdot\nabla\phi) \quad (27)\\&= rJ^{-1}S^1_\phi\end{aligned}$$

where ϕ stands for K or ϵ, S^1_ϕ is the source terms on the right-hand side of Eqs.(4) and (5), and

$$J^{-1} = \frac{\partial(x,y)}{\partial(\xi,\eta)} = x_\xi y_\eta - x_\eta y_\xi \quad (28)$$

$$\begin{aligned}U &= U_1\xi_x + U_2\xi_y\\V &= U_1\eta_x + U_2\eta_y\end{aligned} \quad (29)$$

$$\mu_\phi = R_e^{-1}(\mu + \frac{\mu_t}{\sigma_\phi}) \quad (30)$$

$$\begin{aligned}\nabla\xi\cdot\nabla\phi &= B^1_1\phi_\xi + B^1_2\phi_\eta\\\nabla\eta\cdot\nabla\phi &= B^2_1\phi_\xi + B^2_2\phi_\eta\end{aligned} \quad (31)$$

$$\begin{aligned}B^1_1 &= \xi_x\xi_x + \xi_y\xi_y\\B^1_2 &= \xi_x\eta_x + \xi_y\eta_y\\B^2_1 &= \eta_x\xi_x + \eta_y\xi_y\\B^2_2 &= \eta_x\eta_x + \eta_y\eta_y\end{aligned} \quad (32)$$

In the above equations, U_1 and U_2 are the velocity components along the $x-$ and $y-$coordinates of the reference frame. $r = 1$ for planar and $r = y$ for axisymmetric flows.

Equation (27) can further be written as

$$\begin{aligned}&\partial_t(rJ^{-1}\rho\phi) + \partial_\xi(rJ^{-1}\rho U\phi) + \partial_\eta(rJ^{-1}\rho V\phi)\\&- \partial_\xi(rJ^{-1}\mu_\phi B^1_1\partial_\xi\phi) - \partial_\eta(rJ^{-1}\mu_\phi B^2_2\partial_\eta\phi) \quad (33)\\&= rJ^{-1}S^1_\phi + S^2_\phi\end{aligned}$$

where S^2_ϕ contains cross-derivative terms due to non-orthogonality

$$S^2_\phi = \partial_\xi(rJ^{-1}B^1_2\mu_\phi\partial_\eta\phi) + \partial_\eta(rJ^{-1}B^2_1\mu_\phi\partial_\xi\phi) \quad (34)$$

3.2 Numerical Discretization

Equation (33) is discretized with the finite-volume approach. Integrating Eq.(33) over a typical control volume centered at C (Fig.2) leads to a flux balance equation

$$\int \partial_t(\rho\phi)d\Omega + F_e - F_w + F_n - F_s = \int S_\phi d\Omega \quad (35)$$

where F_i represents the total flux of ϕ across the cell-face $i(= e, w, n$ or $s)$. Each of the surface fluxes F_i contains a convective contribution F^C_i and a diffusive contribution F^D_i, that is

$$F_i = F^C_i + F^D_i \quad (36)$$

Equation (35) involves no approximation and represents a finite-volume analogue of the differential equation, Eq.(33).

Approximation of Convective Terms

The convective contribution in Eq.(36) can be approximated as

$$F^C_i = C_i\phi_i \quad (37)$$

where C_i is the mass flux across the cell-face i, and can be calculated as

$$\begin{aligned}C_w &= (rJ^{-1}\rho U)_w\\C_e &= (rJ^{-1}\rho U)_e\\C_s &= (rJ^{-1}\rho V)_s\\C_n &= (rJ^{-1}\rho V)_n\end{aligned} \quad (38)$$

The calculation of ϕ_i is a key element for the accuracy and stability of numerical solutions. The more accurate schemes tend to be less stable, and vice versa. Here, the second-order accurate HLPA scheme[8] is used to calculate the face value of ϕ. This scheme is implemented in the following deferred correction way proposed by Khosla and Rubin[11]

$$\phi_i = \phi^u_i + \lambda(\phi^{h,l-1}_i - \phi^{u,l-1}_i) \quad (39)$$

where u and h indicate the (first-order accurate) upwind and higher-order schemes, $l-1$ represents the previous iteration level, and λ is a parameter which

blends the two schemes with limiting values $\lambda = 0$ for the upwind and $\lambda = 1$ for the higher-order scheme.

For the upwind scheme

$$\begin{aligned}
\phi_w^u &= U_w^+ \phi_W + U_w^- \phi_C \\
\phi_e^u &= U_e^+ \phi_C + U_e^- \phi_E \\
\phi_s^u &= V_s^+ \phi_S + V_s^- \phi_C \\
\phi_n^u &= V_n^+ \phi_C + V_n^- \phi_N
\end{aligned} \tag{40}$$

where

$$U_i^+ = 1 - U_i^-, \quad U_i^- = \begin{cases} 0, & \text{if } U_i \geq 0 \\ 1, & \text{otherwise} \end{cases} \tag{41}$$

$$V_i^+ = 1 - V_i^-, \quad V_i^- = \begin{cases} 0, & \text{if } V_i \geq 0 \\ 1, & \text{otherwise} \end{cases} \tag{42}$$

For the HLPA scheme

$$\begin{aligned}
\phi_w^h &= U_w^+ \phi_W + U_w^- \phi_C + \Delta\phi_w \\
\phi_e^h &= U_e^+ \phi_C + U_e^- \phi_E + \Delta\phi_e \\
\phi_s^h &= V_s^+ \phi_S + V_s^- \phi_C + \Delta\phi_s \\
\phi_n^h &= V_n^+ \phi_C + V_n^- \phi_N + \Delta\phi_n
\end{aligned} \tag{43}$$

where

$$\begin{aligned}
\Delta\phi_w &= U_w^+ \alpha_w^+ (\phi_C - \phi_W) \frac{\phi_W - \phi_{WW}}{\phi_C - \phi_{WW}} \\
&+ U_w^- \alpha_w^- (\phi_W - \phi_C) \frac{\phi_C - \phi_E}{\phi_W - \phi_E}
\end{aligned} \tag{44}$$

$$\begin{aligned}
\Delta\phi_e &= U_e^+ \alpha_e^+ (\phi_E - \phi_C) \frac{\phi_C - \phi_W}{\phi_E - \phi_W} \\
&+ U_e^- \alpha_e^- (\phi_C - \phi_E) \frac{\phi_E - \phi_{EE}}{\phi_C - \phi_{EE}}
\end{aligned} \tag{45}$$

$$\begin{aligned}
\Delta\phi_s &= V_s^+ \alpha_s^+ (\phi_C - \phi_S) \frac{\phi_S - \phi_{SS}}{\phi_C - \phi_{SS}} \\
&+ V_s^- \alpha_s^- (\phi_S - \phi_C) \frac{\phi_C - \phi_N}{\phi_S - \phi_N}
\end{aligned} \tag{46}$$

$$\begin{aligned}
\Delta\phi_n &= V_n^+ \alpha_n^+ (\phi_N - \phi_C) \frac{\phi_C - \phi_S}{\phi_N - \phi_S} \\
&+ V_n^- \alpha_n^- (\phi_C - \phi_N) \frac{\phi_N - \phi_{NN}}{\phi_C - \phi_{NN}}
\end{aligned} \tag{47}$$

$$\alpha_w^+ = \begin{cases} 1 & \text{if } \left| \dfrac{\phi_C - 2\phi_W + \phi_{WW}}{\phi_C - \phi_{WW}} \right| < 1 \\ 0 & \text{otherwise} \end{cases}$$

$$\alpha_w^- = \begin{cases} 1 & \text{if } \left| \dfrac{\phi_W - 2\phi_C + \phi_E}{\phi_W - \phi_E} \right| < 1 \\ 0 & \text{otherwise} \end{cases} \tag{48}$$

$$\alpha_e^+ = \begin{cases} 1 & \text{if } \left| \dfrac{\phi_E - 2\phi_C + \phi_W}{\phi_E - \phi_W} \right| < 1 \\ 0 & \text{otherwise} \end{cases}$$

$$\alpha_e^- = \begin{cases} 1 & \text{if } \left| \dfrac{\phi_C - 2\phi_E + \phi_{EE}}{\phi_C - \phi_{EE}} \right| < 1 \\ 0 & \text{otherwise} \end{cases} \tag{49}$$

$$\alpha_s^+ = \begin{cases} 1 & \text{if } \left| \dfrac{\phi_C - 2\phi_S + \phi_{SS}}{\phi_C - \phi_{SS}} \right| < 1 \\ 0 & \text{otherwise} \end{cases}$$

$$\alpha_s^- = \begin{cases} 1 & \text{if } \left| \dfrac{\phi_S - 2\phi_C + \phi_N}{\phi_S - \phi_N} \right| < 1 \\ 0 & \text{otherwise} \end{cases} \tag{50}$$

$$\alpha_n^+ = \begin{cases} 1 & \text{if } \left| \dfrac{\phi_N - 2\phi_C + \phi_S}{\phi_N - \phi_S} \right| < 1 \\ 0 & \text{otherwise} \end{cases}$$

$$\alpha_n^- = \begin{cases} 1 & \text{if } \left| \dfrac{\phi_C - 2\phi_N + \phi_{NN}}{\phi_C - \phi_{NN}} \right| < 1 \\ 0 & \text{otherwise} \end{cases} \tag{51}$$

It can be seen that Eq.(43) is in fact the result of the first-order upwinding with an additional term $\Delta\phi_i$ added. The additional term may be viewed as an antidiffusive correction to the upwind scheme.

The performance of the HLPA scheme is demonstrated in Figure 3 for a one-dimensional pure convection of a scalar profile. Figure 3(a) shows the test case: a rectangular S-profile at the initial time t=0 is being transported in the x-direction by an inviscid flow with prescribed velocities U=1 and V=0.

Figure 3(b) shows the computational domain. Calculations were carried out on two uniform grids, one comprising 201×2 and the other 1001×2 grid nodes. Two time increments were used, with Δt=0.4 for the coarse and Δt=0.1 for the fine grid. Figures 3(c) and (d) show the S-profiles at the time t=100 calculated by five different convection schemes: upwind, QUICK[12], SOUCUP[13], HLPA and SMART[14]. It is seen that HLPA captures steep gradients quite well while maintaining the boundedness of the solution, as compared to the other schemes.

Approximation of Diffusive Terms

The diffusive flux in Eq.(36) can be divided into two parts

$$F_i^D = F_i^{DN} + F_i^{DC} \tag{52}$$

The first part F_i^{DN} contains only one term which has the first derivative of ϕ in the direction "normal" to the cell-face i. It can be written as

$$\begin{aligned} F_w^{DN} &= -D_w(\phi_C - \phi_W) \\ F_e^{DN} &= -D_e(\phi_E - \phi_C) \\ F_s^{DN} &= -D_s(\phi_C - \phi_S) \\ F_n^{DN} &= -D_n(\phi_N - \phi_C) \end{aligned} \tag{53}$$

where

$$\begin{aligned} D_w &= (rJ^{-1}B_1^1\mu_\phi)_w \\ D_e &= (rJ^{-1}B_1^1\mu_\phi)_e \\ D_s &= (rJ^{-1}B_2^2\mu_\phi)_s \\ D_n &= (rJ^{-1}B_2^2\mu_\phi)_n \end{aligned} \tag{54}$$

The second part F_i^{DC} involves the cross-derivative terms arising from grid non-orthogonality in Eq.(34). Only the normal derivative diffusive flux, F_i^{DN}, is coupled with the convective flux, F_i^C, to form the main coefficients of the difference equation, while the cross-derivative diffusive flux, F_i^{DC}, is treated explicitly as a pseudo-source term to avoid the possibility of producing negative coefficients in an implicit treatment.

Linearization of Source Terms

The source terms are linearized as

$$S_\phi = S_\phi^P + S_\phi^N \phi_C \tag{55}$$

The coefficients S_ϕ^P and S_ϕ^N are defined such that

$$\begin{aligned} S_\phi^P &\geq 0 \\ S_\phi^N &\leq 0 \end{aligned} \tag{56}$$

This treatment enhances the stability of the numerical process and prevents the calculated value of ϕ from becoming negative, especially in low turbulence regions.

Approximation of Time Derivative

Two time discretization schemes are used to approximate the time derivative appearing in Eq.(35). They are

1) Fully Implicit (FI) scheme of first-order accuracy which gives

$$\partial_t(\rho\phi) = \frac{(\rho\phi)^n - (\rho\phi)^{n-1}}{\Delta t} \tag{57}$$

2) Three-Level Fully Implicit (TLFI) scheme of second-order accuracy which gives

$$\partial_t(\rho\phi) = \frac{3(\rho\phi)^n - 4(\rho\phi)^{n-1} + (\rho\phi)^{n-2}}{2\Delta t} \tag{58}$$

where the superscript n refers to the current time level, and

$$\Delta t = t^n - t^{n-1} \tag{59}$$

Final Form of Discretized Equations

After replacing all the terms in Eq.(35) by their discretized analogues, we obtain the following difference equation which relates the principal unknown ϕ_C to its four neighbours $\phi_i (i = W, E, S, N)$

$$\begin{aligned} A_C\phi_C = A_E\phi_E + A_W\phi_W + A_N\phi_N + A_S\phi_S \\ + S_P \end{aligned} \tag{60}$$

where

$$\begin{aligned} A_E &= D_e - C_eU_e^- \\ A_W &= D_w + C_wU_w^+ \\ A_N &= D_n - C_nV_n^- \\ A_S &= D_s + C_sV_s^+ \\ A_C &= A_E + A_W + A_N + A_S - S_N \end{aligned} \tag{61}$$

$$S_P = S_P^1 + \max(0,\ S_\phi^2) + S_\phi^3 + S_P^4$$
$$S_N = S_N^1 + \min(0,\ S_\phi^2/\phi) + S_N^4 \tag{62}$$

where, S_P^1 and S_N^1 are the coefficients of the source term S_ϕ^1,

For the K-equation (ϕ=K):

$$S_P^1 = rJ^{-1}[\max(0,\ P) + \max(0,\ D)]$$
$$S_N^1 = rJ^{-1}[\min(0,\ P) + \min(0,\ D) - \rho\epsilon]/K \tag{63}$$

For the ϵ-equation (ϕ=ϵ):

$$S_P^1 = rJ^{-1}[\max(0,\ f_1C_1P/K)\epsilon + \max(0,\ E)]$$
$$S_N^1 = rJ^{-1}[\min(0,\ f_1C_1P/K) + \min(0,\ E)/\epsilon - f_2C_2\rho\epsilon/K] \tag{64}$$

S_ϕ^2 is calculated by Eq.(34), S_ϕ^3 contains the deferred correction part in Eq.(39)

$$S_\phi^3 = -\lambda[C_e(\phi_e^h - \phi_e^u) - C_w(\phi_w^h - \phi_w^u) + C_n(\phi_n^h - \phi_n^u) - C_s(\phi_s^h - \phi_s^u)] \tag{65}$$

S_P^4 and S_N^4 are due to the use of

FI scheme (Eq. 57):

$$S_P^4 = \frac{rJ^{-1}\rho}{\Delta t}\phi_C^{n-1}$$
$$S_N^4 = -\frac{rJ^{-1}\rho}{\Delta t} \tag{66}$$

TLFI scheme (Eq. 58):

$$S_P^4 = \frac{rJ^{-1}\rho}{\Delta t}(2\phi_C^{n-1} - 0.5\phi_C^{n-2})$$
$$S_N^4 = -1.5\frac{rJ^{-1}\rho}{\Delta t} \tag{67}$$

In formulating Eq.(60), the convection terms calculated by the upwind scheme are coupled with the normal diffusion terms to form the main coefficients A_i. By this approach, the positivity of all the main coefficients is ensured so that the resulting coefficient matrix will be always diagonally dominant.

3.3 Calculation Sequence

The sequence in which the calculation is carried out is as follows:

a. Initialize all field values.

b. Solve the U_1- and U_2-momentum equations using the NPARC code.

c. Update the boundary conditions for the turbulent quantities.

d. Solve the K-equation.

e. Solve the ϵ-equation.

f. Update the turbulent eddy viscosity μ_t.

g. Return to step b.

The sequence of steps b to g are repeated until the convergence criterion is satisfied. The system of equations (60) are solved with the alternating direction TDMA of Thomas.

4. Description of the Module

To facilitate identification, all the subroutine names in the module start with CM. In order to use the module, the user only needs to call its two subroutines: CMA0 and CMTURB, in the NPARC code.

4.1 Subroutine CMA0

The subroutine CMA0 is for setting up the parameters of the module. It contains the following arguments:

JMAX,KMAX,NMAX,NTURB,IAXISY,RE,
NJPAT,JPJ2,JPJM,JPK2,JPKM,
NKPAT,KPJ2,KPJM,KPK2,KPKM,
NJSEG,JLINE,JKLOW,JKHIGH,JTYPE,
JSIGN,JEDGE,
NKSEG,KLINE,KJLOW,KJHIGH,KTYPE,
KSIGN,KEDGE

These are all the variables already used in the NPARC code to define flow, geometric and boundary conditions. In addition, it has the following user-specified parameters:

BDMAX(i), BDMIN(i) — Upper and lower bounds for the values of K (i=1), ϵ (i=2) and μ_t (i=3). These bounds are introduced for numerical purposes only, that is, to prevent the corresponding turbulence quantities from becoming negative or abnormally large during the solution process. Currently, they are set to

BDMAX(1)=1.0E+6
BDMAX(2)=1.0E+6
BDMAX(3)=5.0E+3
BDMIN(1)=1.0E-8

BDMIN(2)=1.0E-8
BDMIN(3)=1.0E-3
These should cover a wide range of the physically meaningful values of K, ϵ and μ_t. It is to be noted that these values are only valid for the non-dimensional turbulence quantities, as defined in the NPARC code.

FDEFER — Blending factor λ defined in Eq.(39). Its value may vary from 0 to 1 with the limiting value 0 for the upwind and 1 for the HLPA scheme. The solution tends to be more stable, but also more diffusive when this factor is reduced.

MODELS — Turbulence model selector with 1 for Chien, 2 for Shih-Lumley and 3 for CMOTT models. The Baldwin-Lomax model is used when NC is less than NTURB, which is defined in and is consistent with the NPARC code.

RELAX(i) — Under-relaxation factors for K (i=1) and ϵ (i=2). Currently, they are set to
RELAX(1)=0.8
RELAX(2)=0.8
Should unstability occur, try to reduce these values.

The subroutine CMA0 needs to be called only once in the NPARC code. Currently, it is called in the subroutine INITIA as shown below

```
      SUBROUTINE  INITIA
      ......
      DO 210 MB=1,NBLOCK
      ......
      CALL CMA0(···)
210   CONTINUE
      ......
      END
```

4.2 Subroutine CMTURB

This is the major interface between the NPARC and module. The user may simply replace all CALL MUTURB by CALL CMTURB in NAPRC. The subroutine MUTURB calls all turbulence model subroutines in NPARC.

5. References

1. Chien, K.Y., "Predictions of channel and boundary-layer flows with a low Reynolds number turbulence model," *AIAA Journal*, Vol.20, 1982, pp.33-38.
2. Georgiadis, N.J., Chitsomboon, T. and Zhu, J., "Modification of the two-equation turbulence model in NPARC to a Chien low Reynolds number K-ϵ formulation," NASA TM 106710, 1994.
3. Shih, T.-H., and Lumley, J.L., "Kolmogorov behavior of near-wall turbulence and its application in turbulence modeling," *Comp. Fluid Dyn.*, Vol.1, 1993, pp.43-56.
4. Launder, B.E., and Spalding, D.B., "The numerical computation of turbulent flows," *Computer Methods in Applied Mechanics and Engineering*, Vol.3, 1974, pp.269-289.
5. Patel, V.C., Rodi, W. and Scheuerer, G., "Turbulence models for near wall and low Reynolds number flows: a review," *AIAA Journal*, Vol.23, 1985, pp.1308-1319.
6. Shih, T.-H., Zhu, J. and Lumley, J.L., "A new Reynolds stress algebraic equation model," NASA TM 106644, 1994, also to appear in *Computer Methods in Applied Mechanics and Engineering.*
7. Shih, T.-H., Liou, W.W., Shabbir, A., Yang, Z. and Zhu, J., "A new K-ϵ eddy viscosity model for high Reynolds number turbulent flows - Model development and validation," NASA TM 106721, 1994, also in *Computers and Fluids*, Vol.24, No.3, 1995, pp.227-238.
8. Zhu, J., "A low diffusive and oscillation-free convection scheme," *Communications in Applied Numerical Methods.*, Vol.7, 1991, pp.225-232.
9. Zhu, J., "On the higher-order bounded discretization schemes for finite-volume computations of incompressible flows ," *Computer Methods in Applied Mechanics and Engineering*, Vol.98, 1992, pp.345-360.
10. Yang, Z., Georgiadis, N.J., Zhu, J. and Shih, T.-H., "Calculations of inlet/nozzle flows using two new K-ϵ model," AIAA-95-2761, presented at the 31st AIAA/ASME/SAE/ASEE Joint Propulsion Conference and Exhibit, July 1995, San Diego, CA.
11. Khosla, P.K. and Rubin, S.G., "A diagonally dominant second-order accurate implicit scheme," *Computers and Fluids*, Vol.2, 1974, pp.207-209.
12. Leonard, B.P., "A stable and accurate convective modelling procedure based on quadratic upstream interpolation," *Computer Methods in Applied Mechanics and Engineering*, Vol.19, 1979, pp.59-98.
13. Zhu, J. and Rodi, W., "A low dispersion and bounded convection scheme," *Computer Methods in Applied Mechanics and Engineering*, Vol.92, 1991, pp.87-96.
14. Gaskell, P.H., and Lau, A.K.C., "Curvature-compensated convective transport: SMART, A new boundedness preserving transport algorithm," *International Journal for Numerical Methods in Fluids*, Vol.8, 1988, pp.617-641.

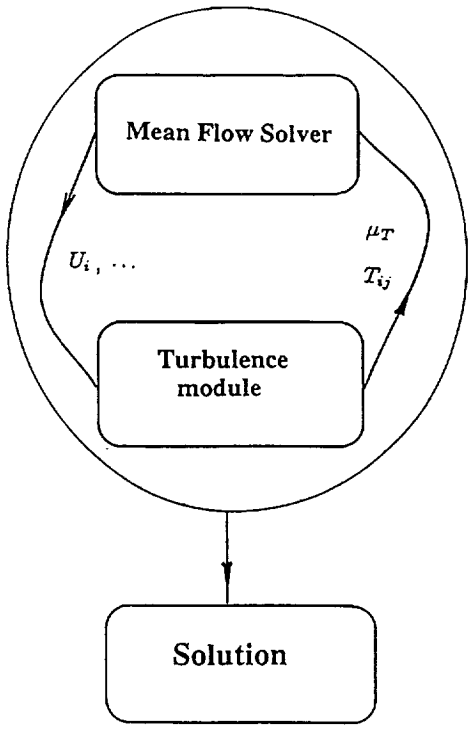

Fig.1 Interaction between the mean flow solver and the turbulence module

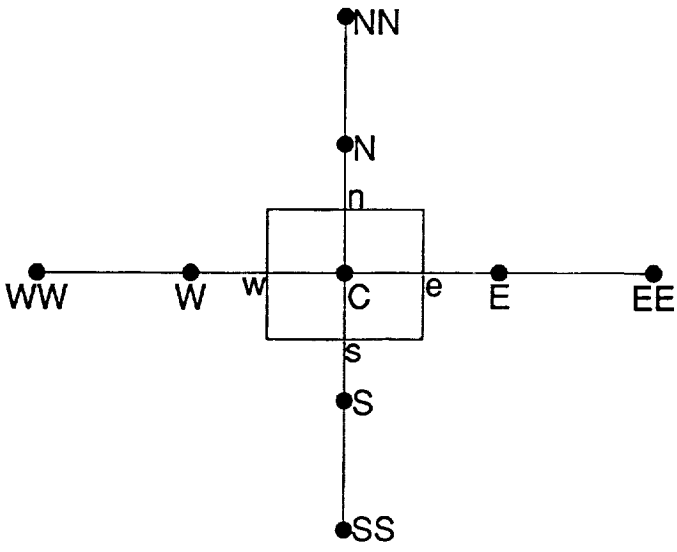

Fig.2 A typical control volume centered at node C and its neighbouring nodes

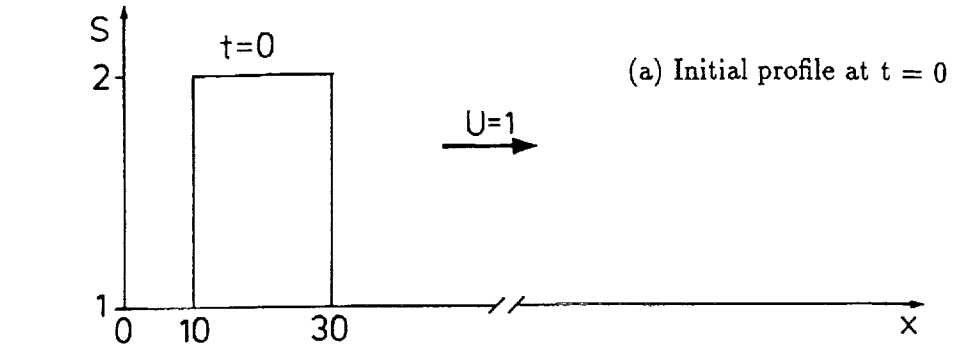

(a) Initial profile at t = 0

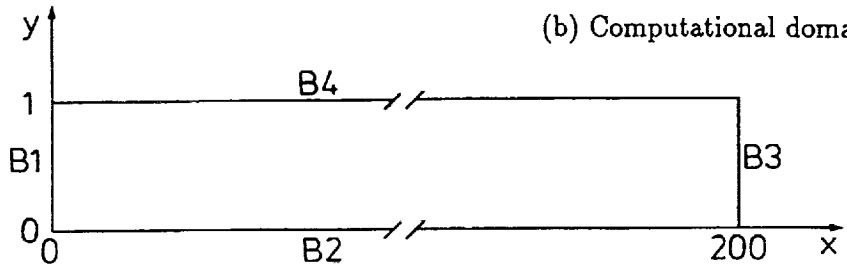

(b) Computational domain

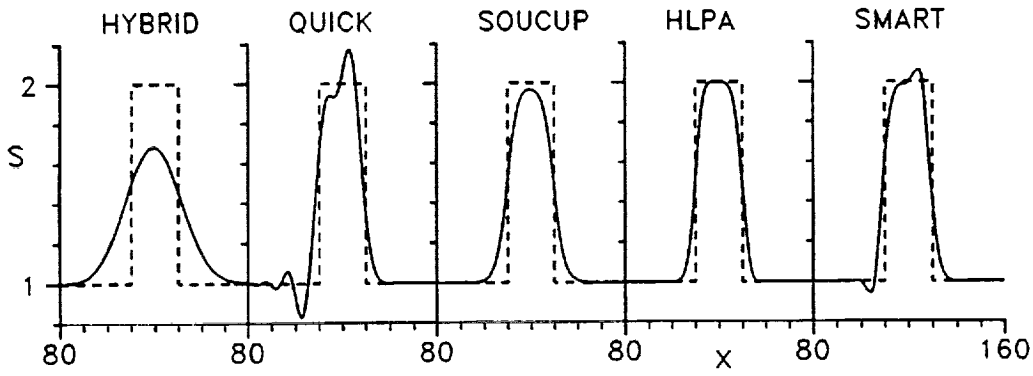

(c) Predicted profiles at t = 100 (201×2 grid, $\Delta t = 0.4$)

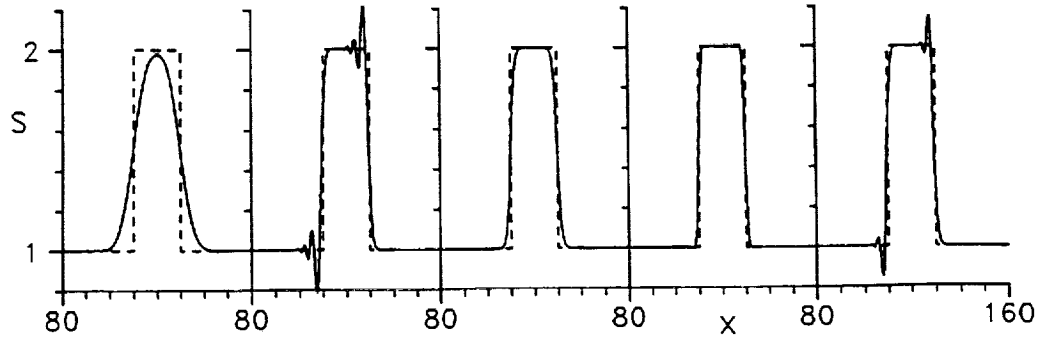

(d) Predicted profiles at t = 100 (1001×2 grid, $\Delta t = 0.1$)

Fig.3 Pure convection of a scalar profile

REPORT DOCUMENTATION PAGE

Form Approved
OMB No. 0704-0188

1. AGENCY USE ONLY (*Leave blank*)	2. REPORT DATE	3. REPORT TYPE AND DATES COVERED
	June 1995	Contractor Report

4. TITLE AND SUBTITLE

A Turbulence Module for the NPARC Code

5. FUNDING NUMBERS

WU-505-90-5K
NCC3-370

6. AUTHOR(S)

J. Zhu and T.-H. Shih

7. PERFORMING ORGANIZATION NAME(S) AND ADDRESS(ES)

Institute for Computational Mechanics in Propulsion
22800 Cedar Point Road
Cleveland, Ohio 44142

8. PERFORMING ORGANIZATION REPORT NUMBER

E-9745

9. SPONSORING/MONITORING AGENCY NAME(S) AND ADDRESS(ES)

National Aeronautics and Space Administration
Lewis Research Center
Cleveland, Ohio 44135-3191

10. SPONSORING/MONITORING AGENCY REPORT NUMBER

NASA CR-198358
ICOMP-95-12
CMOTT-95-1
AIAA-95-2612

11. SUPPLEMENTARY NOTES

Prepared for the 31st Joint Propulsion Conference and Exhibit cosponsored by AIAA, ASME, SAE, and ASEE, San Diego, California, July 10-12, 1995. J. Zhu and T.-H. Shih Institute for Computational Mechanics in Propulsion and Center for Modeling of Turbulence and Transition, NASA Lewis Research Center (work funded under NASA Cooperative Agreement NCC3-370). ICOMP Program Director, Louis A. Povinelli, organization code 2600, (216) 433-5818.

12a. DISTRIBUTION/AVAILABILITY STATEMENT

Unclassified - Unlimited
Subject Category 64

This publication is available from the NASA Center for Aerospace Information, (301) 621-0390.

12b. DISTRIBUTION CODE

13. ABSTRACT (*Maximum 200 words*)

A turbulence module is developed for the 2D version of the NPARC code which is currently restricted to planar or axisymmetric flows without swirling. Four turbulence models have been built into the module: Baldwin-Lomax, Chien, Shih-Lumley and CMOTT models. The first is a mixing-length eddy-viscosity model which is mainly used for initialization of computational fields and the last three are the low Reynolds number two-equation models. Unlike Chien's model, both the Shih-Lumley and CMOTT models do not involve the dimensionless wall distance y^+, an advantage for separated flow calculations. Contrary to the NPARC and most other compressible codes, the non-delta form of transport equations is used which leads to a simpler linearization and is more effective than using the delta form in ensuring the positiveness of the turbulent kinetic energy and its dissipation rate. To reduce numerical diffusion while maintaining necessary stability, a second-order accurate and bounded scheme is used for the convective terms of the turbulent transport equations. This scheme is implemented in a deferred correction manner so that the main coefficients of the resulting difference equations are always positive, thus making the numerical solution process unconditionally stable. The system of equations are solved via a decoupled method and by the alternating direction TDMA of Thomas. The module can be easily linked to the NPARC code for turbulent flow calculations.

14. SUBJECT TERMS	15. NUMBER OF PAGES
Turbulence models; NPARC code; Propulsion flows; Turbulence module	12
	16. PRICE CODE: A03

17. SECURITY CLASSIFICATION OF REPORT	18. SECURITY CLASSIFICATION OF THIS PAGE	19. SECURITY CLASSIFICATION OF ABSTRACT	20. LIMITATION OF ABSTRACT
Unclassified	Unclassified	Unclassified	